

# Bilayer Molecular Electronics: All-Carbon Electronic Junctions Containing Molecular Bilayers Made with “Click” Chemistry

Sayed Youssef Sayed,<sup>†,‡,§,||</sup> Akhtar Bayat,<sup>†,‡,§</sup> Mykola Kondratenko,<sup>†,‡</sup> Yann Leroux,<sup>⊥</sup> Philippe Hapiot,<sup>⊥</sup> and Richard L. McCreery<sup>\*,†,‡</sup>

<sup>†</sup>Department of Chemistry, University of Alberta, Edmonton, Alberta T6G 2G2, Canada

<sup>‡</sup>National Institute for Nanotechnology, National Research Council Canada, Edmonton, Alberta T6G 2M9, Canada

<sup>⊥</sup>Institut des Sciences Chimiques de Rennes 1 (Equipe MaCSE), CNRS, UMR 6226, Université de Rennes, 35042 Rennes Cedex, France

**S** Supporting Information

**ABSTRACT:** Bilayer molecular junctions were fabricated by using the alkyne/azide “click” reaction on a carbon substrate, followed by deposition of a carbon top contact in a crossbar configuration. The click reaction on an alkyne layer formed by diazonium reduction permitted incorporation of a range of molecules into the resulting bilayer, including alkane, aromatic, and redox-active molecules, with high yield (>90%) and good reproducibility. Detailed characterization of the current–voltage behavior of bilayer molecular junctions indicated that charge transport is consistent with tunneling, but that the effective barrier does not strongly vary with molecular structure for the series of molecules studied.

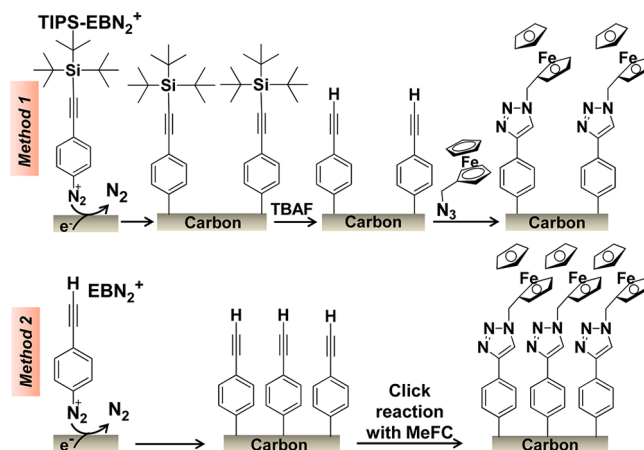
One of the major motives for the development of molecular electronics is the wide variety of molecular structures available and the unusual electronic behaviors expected for different molecules. Robust methods for bonding molecules to electrode surfaces and immobilizing different functional entities are among the challenges encountered in the field. Electro-reduction of aryl diazonium salts on carbon surfaces followed by vapor deposition of copper or carbon produced stable and reproducible molecular junctions, which exhibit strong electronic coupling through a covalent carbon–carbon bond between the substrate and nanoscopic molecular layers (2–22 nm thick).<sup>1,2</sup> However, the requirement of an aromatic diazonium reagent somewhat limits the range of molecules available, and often results in multilayers with attendant necessity of verifying layer thickness with atomic force microscopy (AFM).<sup>3</sup> Herein we report the use of the alkyne–azide “click” reaction to prepare covalently bonded molecular bilayers, which may include alkane, aromatic, and redox moieties, some of which are not possible with solely diazonium chemistry. We demonstrate high-yield and reproducible carbon/bilayer/carbon molecular junctions formed by click chemistry on a diazonium-derived “primer” layer, and investigate their dependence on molecular structure and temperature. Ultraviolet photoelectron spectroscopy (UPS) was used to probe the energy levels of the modified carbon substrates, notably the difference between the highest occupied molecular orbital (HOMO) level and the Fermi level ( $E_f -$

$E_{\text{HOMO, onset}}$ ).<sup>4</sup> Strong coupling between the bilayer and carbon contacts results in the formation of an overall new system with its own characteristic energy level alignments and tunneling barrier, which in turn control charge transport.

The Huisgen 1,3-dipolar cycloaddition of azides and alkynes to produce 1,2,3-triazoles is one of the most efficient click reactions.<sup>5,6</sup> In addition to being amenable to a wide range of molecules, azide–alkyne click chemistry is self-limiting and not prone to multilayer formation. Consequently, click chemistry has been used in a variety of applications, including micro-contact printing,<sup>7</sup> polymer<sup>8</sup> and biomedical<sup>9</sup> synthesis, and the fabrication of solar<sup>10</sup> and OLED<sup>11</sup> devices.

Two-step diazonium/click modification of carbon electrodes has been demonstrated, resulting in high coverage of ferrocene (Fc) on glassy carbon.<sup>12</sup> First, a molecular layer with a functional group is electrografted on carbon surfaces via reduction of an aryldiazonium reagent, as shown in Scheme 1, method 1. The precursor 4-((triisopropylsilyl)ethynyl)benzenediazonium salt (TIPS-EBN<sub>2</sub><sup>+</sup>) was found to impede the production of multilayers and form a reactive ethynylbenzene monolayer after deprotection of the bulky silyl groups.<sup>12</sup>

**Scheme 1. Different Modification Pathways for Formation of Molecular Bilayers via Click Chemistry**



Received: July 4, 2013

The azide–alkyne click reaction was then used to produce the Fc-modified surface shown in the upper right of Scheme 1, which exhibited the expected Fc voltammetry in electrolyte solution.

We applied the TIPS/click procedures to modify pyrolyzed photoresist film (PPF) surfaces, and then prepared large-area ( $\sim 0.0013 \text{ cm}^2$ ) molecular junctions by deposition of e-beam carbon (e-C) and Au. TIPS-EB junctions show high and nearly linear conductivity ( $3.4 \text{ A cm}^{-2}$  at 50 mV) (Figure S1, Supporting Information), indicating direct contact between the PPF and e-C layers. Click reactions of different azide molecules on deprotected TIPS-EB surfaces resulted in junctions showing similar short circuits, probably due to the existence of pinholes in the initial EB layer following hydrolysis of the bulky silane protecting group (method 1 in Scheme 1). A less bulky substituent, trimethylsilyl (TMS), on the ethynylbenzene  $\text{N}_2^+$  moieties should decrease the pinhole density. However, junctions obtained by reduction of TMS-EB- $\text{N}_2^+$  followed by deprotection and e-C deposition also exhibited direct contact between PPF and e-C, implying a porous molecular layer (Figure S2).

An alternative approach is shown in Scheme 1, method 2, in which an initial ethynylbenzene “primer” layer is formed by electroreduction of ethynylbenzene diazonium ion on PPF followed by click coupling to azidomethylferrocene (MeFc). As shown in the Supporting Information, AFM indicates an EB layer thickness of  $2.2 \pm 0.5 \text{ nm}$ , indicating a multilayer of 3–4 molecules terminated by an ethynyl group. The AFM root-mean-square (rms) roughness increases slightly from 0.26 nm for unmodified PPF to 0.43 nm for the PPF/EB, indicating good thickness uniformity (Figure S3). We reported previously that similar EB multilayers could be incorporated into PPF/EB/Cu molecular junctions, with behavior similar to that of other aromatic molecules.<sup>1</sup> Click modification of the EB layer with MeFc yielded a total layer thickness of  $3.4 \pm 0.6 \text{ nm}$ , also with minimal change in rms roughness. Attachment of Fc to the EB layer was confirmed by X-ray photoelectron spectroscopy, showing  $\text{Fe}_{2p}$  peaks at 707 and 721 eV, representative of  $\text{Fe}^{2+}$  in Fc (Figure S4).<sup>13</sup> The ferrocene/ferrocenium electrochemical redox behavior for immobilized system on PPF was confirmed by cyclic voltammetry (Figure S5), revealing high Fc coverage of  $\sim 4.3 \times 10^{-10} \text{ mol cm}^{-2}$ .

Figure 1 shows the current density vs bias voltage ( $J$ – $V$ ) curves for PPF/molecule/e-C(10 nm)/Au(15 nm) molecular junctions containing EB alone or EB modified with methylphenylazide (EB-MePh), MeFc, and hexylferrocene azide (HxFc). Detailed statistics are provided in Table S1, but the overall yield for 96 junctions on 16 samples was 95% of non-short-circuited devices, with the relative standard deviation of the current at 0.1 V ranging from 1.2% to 26%. Figure S6 shows an overlay of 15 junctions for EB-HxFc from two samples. Moreover, the  $J$ – $V$  curves show only a small decrease in current density after exposure to ambient air for 8 months. These findings are similar to the results observed from diazonium-derived molecular devices,<sup>14</sup> and clearly indicate that bilayer devices may be fabricated with high yield.

Diverse aromatic compounds strongly coupled to PPF surfaces were found to result in a modest span ( $< 0.3 \text{ eV}$  from  $J$ – $V$  measurements) of the tunneling barrier with an average of 1.2 eV, statistically distinguishable from the 2.0 eV average tunneling barrier for alkanes.<sup>1</sup> In order to modulate the charge transport of the functioning molecular junction, we coupled the EB layer (by click chemistry) with three different

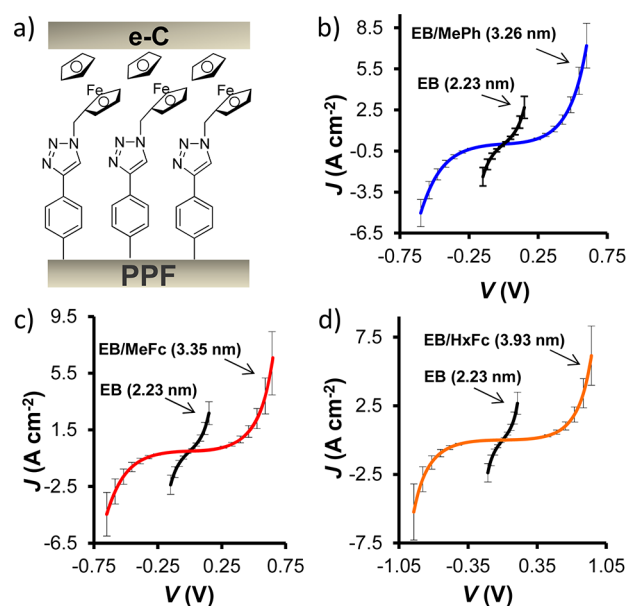


**Figure 1.** (a) Schematic of carbon/bilayer/evaporated carbon junction. Overlay of  $J$ – $V$  curves for EB and EB after click coupling with methylphenyl (a), methylferrocene (b), and hexylferrocene (c) moieties. Each curve is an average of four junctions, with error bars equaling  $\pm 1$  standard deviation.

alkanes: azidooctane ( $\text{C}_8$ ), azidododecane ( $\text{C}_{12}$ ), and azidohexadecane ( $\text{C}_{16}$ ). Figure 2 shows  $J$ – $V$  curves from EB-triazole-

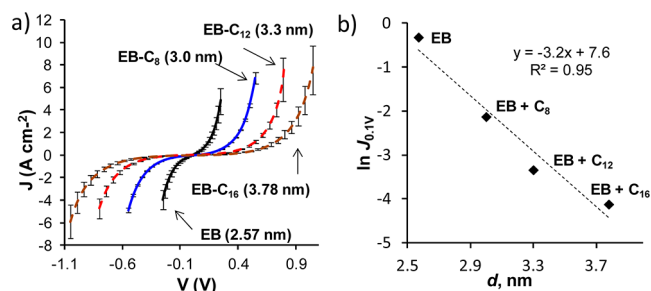


**Figure 2.** Overlay of  $J$ – $V$  curves for EB and EB coupled with  $\text{C}_8$ ,  $\text{C}_{12}$ , and  $\text{C}_{16}$  moieties by click chemistry: (a) attenuation plot and (b)  $\ln J_{0.1V}$  versus thickness ( $d$ ) of alkane junctions.

alkane bilayer junctions containing 8, 12, and 16 methylene groups. It is reasonable to assume that the triazole/alkane layer is one molecule thick, given the self-limiting nature of the alkyne/azide reaction.

The bilayer thicknesses measured with AFM were  $3.0 \pm 0.6$ ,  $3.3 \pm 0.6$ , and  $3.8 \pm 0.5 \text{ nm}$  for  $\text{C}_8$ ,  $\text{C}_{12}$ , and  $\text{C}_{16}$ , respectively. Note that the alkane layer is likely disordered and not necessarily in an all-trans configuration.  $J$ – $V$  curves for EB/alkane bilayers are shown in Figure 2, with statistics provided in Table S1.

The current density decreases monotonically with alkane layer thickness, with a roughly linear plot of  $\ln J$  vs bilayer thickness (Figure 2b) having a slope of  $\sim 3.2 \text{ nm}^{-1}$ . The  $J$ – $V$  curves for the EB/alkane, EB/Fc, and EB/MePh junctions were all nearly symmetric, with rectification ratios ( $|J_+/J_-|$ ) of less than 1.4 at  $\pm 0.6 \text{ V}$ . Figure 3 shows a composite attenuation plot for the bilayer junctions as well as results for nitroazobenzene devices made with both Cu and e-C top contacts. Note that the magnitudes of the current densities are comparable for similar

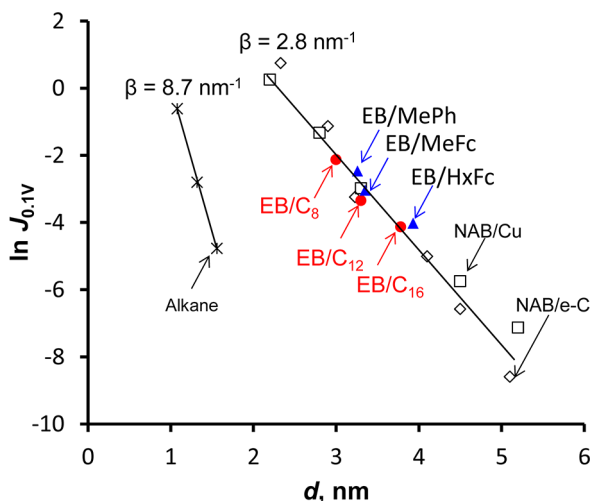


**Figure 3.** Overlay of selected attenuation plots for aromatic, aliphatic, and bilayer molecules in ensemble molecular junctions. NAB = nitroazobenzene with Cu or e-beam carbon contacts, alkane with Au top contact. Alkane/Au data are from ref 20. Solid lines are the least-squares fits for the aromatic and aliphatic devices with the indicated slopes.

thicknesses for the entire range of molecules, and the slopes of the attenuation plots are all close to  $3 \text{ nm}^{-1}$ .

The temperature dependence of the  $J$ - $V$  curves was determined between 100 and 400 K to investigate the charge transport mechanism. Figure 4a,b shows  $J$ - $V$  curves for EB/ $C_{12}$

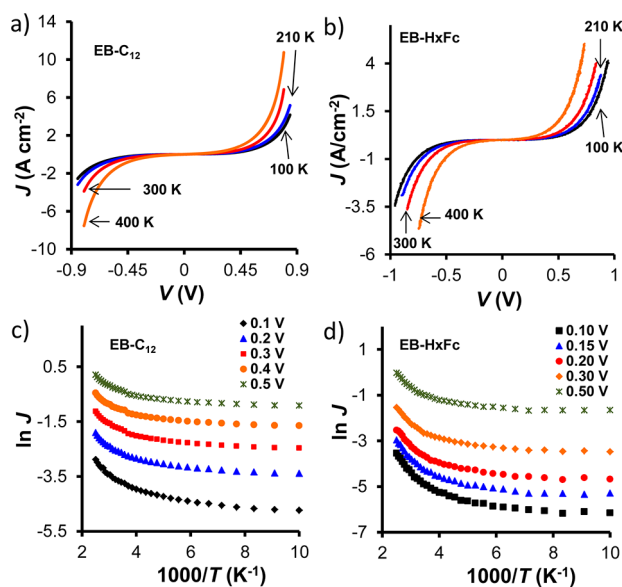


**Figure 4.**  $J$ - $V$  curves at 100, 210, 300, and 400 K for (a) EB- $C_{12}$  and (b) EB-HxFc junctions. Arrhenius plots of  $\ln J$  vs  $1000/T$  for (c) EB- $C_{12}$  and (d) EB-HxFc junctions.

and EB/HxFc junctions, respectively, with corresponding Arrhenius plots in Figure 4c,d. Figures S8 and S9 provide Arrhenius plots for MePh and MeFc junctions, and Table S2 presents the apparent Arrhenius slopes at various voltages and temperature ranges. Although the temperature dependence is weak for the entire 100–400 K range, two approximately linear Arrhenius regions are observed at high (300–400 K) and low (100–210 K)  $T$ . Nearly temperature-independent conductance

is observed from 100 to 210 K, with apparent activation energies ( $E_a$ ) ranging from 2 to 8 meV, while for 300–400 K,  $E_a$  values ranged from 32 to 114 meV. The appearance and slopes of the Arrhenius plots are quite similar to those observed for PPF/molecule/e-C devices based on diazonium reduction without click chemistry.<sup>15</sup> The low activation energies at low temperatures are consistent with a quantum tunneling transport mechanism.<sup>2,14</sup> The highest  $E_a$ , observed at 300–400 K (114 meV for HxFc), is significantly smaller than that expected for a redox hopping mechanism (0.35–0.64 eV),<sup>2,16</sup> and may be due to the broadened Fermi function of the carbon contacts.<sup>17</sup>

Frisbie et al.<sup>4</sup> used UPS of the substrate/molecule surface (without top contact) to determine the onset of photoemission from the HOMO relative to the system Fermi level, i.e.,  $E_{\text{HOMO,onset}}$ . This technique applied to PPF modified by diazonium reduction indicated that  $E_{\text{HOMO,onset}}$  for eight different aromatic molecules was “compressed” to a relatively narrow range of  $1.3 \pm 0.2 \text{ eV}$ , while that of an alkane on PPF was  $2.0 \pm 0.1 \text{ eV}$ .<sup>1</sup> UPS spectra of the PPF/EB, PPF/EB- $C_8$ , PPF/EB- $C_{12}$ , and PPF/EB- $C_{16}$  indicated  $E_{\text{HOMO,onset}}$  values in the range of  $1.20 \pm 0.04$ – $1.28 \pm 0.04 \text{ eV}$ , indicating little effect of the alkane on the UPS emission. Furthermore, the  $E_{\text{HOMO,onset}}$  and attenuation constants for the EB-triazole-alkane series are very similar to those observed for molecular layers derived from reduction of aromatic diazonium reagents without subsequent click chemistry.

The high yield and good reproducibility of the bilayer devices studied here should significantly increase the range of molecules amenable to incorporation into molecular junctions, with the current examples including aliphatic, aromatic, and redox-active bilayers. Both the EB and triazole molecular layers are less ordered than Au/thiol self-assembled monolayers, but the resulting molecular junctions are more temperature tolerant and have long operating lifetimes. While the click reaction is self-limiting at one molecular layer, the EB layer preparation is not, and we continue to investigate self-limiting reactions with sufficiently low pinhole density to fabricate bilayer junctions from two self-limited molecular layers. Although there is a possibility of vapor-deposited e-carbon penetrating the triazole layer to make direct contact with the EB layer and the nature of the alkane/e-C contact is uncertain, the EB/alkane series of Figure 2a is evidence that such penetration is not a major factor. The monotonic decrease in current density with alkane length by a factor of  $>30$  is difficult to explain if the response were dominated by direct EB/e-C contacts, and the reproducibility of current magnitude for a range of devices is unlikely for pinhole conduction.

The similarity of the  $J$ - $V$  responses for the range of molecules shown in Figure 3 was unexpected, given the fact that the various bilayers include alkane and aromatic fragments, and a redox center. Nijhuis et al. reported rectification in Fc-containing molecular junctions when the Fc was positioned closer to one contact than the other,<sup>18</sup> structurally similar to the HxFc case reported here. As already noted, our group reported a tunneling barrier of 1.2 eV for aromatic junctions made with diazonium chemistry, and 2.0 eV for aliphatic junctions made by primary amine oxidation.<sup>1</sup> The EB-triazole-alkane bilayer devices reported here could be considered to contain two tunneling barriers of different heights for the aliphatic and aromatic segments, yet they exhibit similar current magnitudes and  $\beta$  values to devices containing only conjugated structures without alkanes. Furthermore, the redox activity of Fc appears to have no effect on symmetry or current magnitude, since the

Fc-containing structures lie on the same attenuation line as non-redox-active MePh and alkanes (Figure 3). We also note that Yoon et al.<sup>19</sup> observed very similar  $J$ - $V$  curves for 13 molecules of similar length but with a range of structures, including thiophene, pyridine, aromatic, and aliphatic segments.

All of the bilayers reported here have total thicknesses determined by AFM of <5.0 nm, well within the range where coherent tunneling is possible for aromatic molecules.<sup>1,2,15</sup> The results indicate that the alkane segment in the EB-triazole-alkane bilayers does indeed decrease the current density, but the observed  $\beta$  for the triazole-alkane series of  $\sim 3 \text{ nm}^{-1}$  (Figure 2b) is smaller than that typically observed for alkanes alone, i.e.,  $8\text{--}9 \text{ nm}^{-1}$ .<sup>20</sup> A possible reason is that the EB-alkane bilayers are comprised of conjugated structures for >70% of their total thickness, so that the tunneling barrier is dominated by the conjugated section. Using the average barrier model of Simmons as a first approximation, the length-weighted barrier height increases from 1.2 to 1.4 eV with the addition of  $\text{C}_{12}$  to EB (Figure S15b), which is within the experimental error of our measurements. It is likely that attempts to model the bilayer as a combination of two tunneling barriers are insufficient, and we are currently conducting detailed calculations with density functional theory to determine the factors affecting the barrier height. The UPS results showing minimal effect of the alkane on photoemission and similar  $E_{\text{HOMO, onset}}$  values for EB and EB-triazole-alkane could reflect a narrow range of tunneling barriers, or that photoemission is predominantly from the orbitals of the aromatic EB layer.

To summarize, in this study we demonstrated that the self-limiting characteristic of click chemistry enabled the construction of various bilayer junctions with a monolayer of the second functional moiety, with high yield and reproducibility. The covalent carbon-carbon bond between the PPF and the EB layer and the covalent bonding between the EB layer and the monolayer formed by click reaction resulted in the formation of a new system with a unique set of energy level alignments. The similarity of charge transport characteristics of bilayer molecular junctions containing EB-alkane ( $\text{C}_8\text{--}\text{C}_{16}$ ), EB-MeFc, EB-HxFc, and EB-MePh molecular layers is consistent with a tunneling mechanism governed by an average barrier height, resulting in a symmetric  $J$ - $V$  curve.

## ■ ASSOCIATED CONTENT

### 📄 Supporting Information

Description of the experimental setup, calibration, optical spectra, molecular layer thickness measurements, assessments of reproducibility, and other details. This material is available free of charge via the Internet at <http://pubs.acs.org>.

## ■ AUTHOR INFORMATION

### Corresponding Author

richard.mccreery@ualberta.ca

### Present Address

<sup>||</sup>S.Y.S.: Chemistry Department, Faculty of Science, Cairo University, Cairo, Egypt

### Author Contributions

<sup>§</sup>S.Y.S. and A.B. contributed equally.

### Notes

The authors declare no competing financial interest.

## ■ ACKNOWLEDGMENTS

This work was supported by the University of Alberta, the National Research Council, the Natural Science and Engineering Research Council of Canada, and Alberta Innovates Technology Futures. We thank Dr. Adam Bergren for valuable discussions.

## ■ REFERENCES

- (1) Sayed, S. Y.; Fereiro, J. A.; Yan, H.; McCreery, R. L.; Bergren, A. *J. Proc. Natl. Acad. Sci. U.S.A.* **2012**, *109*, 11498–11503.
- (2) Yan, H.; Bergren, A. J.; McCreery, R.; Della Rocca, M. L.; Martin, P.; Lafarge, P.; Lacroix, J. C. *Proc. Natl. Acad. Sci. U.S.A.* **2013**, *110*, 5326–5330.
- (3) Anariba, F.; DuVall, S. H.; McCreery, R. L. *Anal. Chem.* **2003**, *75*, 3837–3844.
- (4) Kim, B.; Choi, S. H.; Zhu, X. Y.; Frisbie, C. D. *J. Am. Chem. Soc.* **2011**, *133*, 19864–19877.
- (5) Bock, V. D.; Hiemstra, H.; van Maarseveen, J. H. *Eur. J. Org. Chem.* **2006**, *2006*, 51–68.
- (6) Appukkuttan, P.; Dehaen, W.; Fokin, V. V.; Van der Eycken, E. *Org. Lett.* **2004**, *6*, 4223–4225.
- (7) Rozkiewicz, D. I.; Jańczewski, D.; Verboom, W.; Ravoo, B. J.; Reinhoudt, D. N. *Angew. Chem., Int. Ed.* **2006**, *45*, 5292–5296.
- (8) Wang, M.; Das, M. R.; Li, M.; Boukherroub, R.; Szunerits, S. *J. Phys. Chem. C* **2009**, *113*, 17082–17086.
- (9) Gupta, S.; Schade, B.; Kumar, S.; Böttcher, C.; Sharma, S. K.; Haag, R. *Small* **2013**, *9*, 894–904.
- (10) Cardiel, A. C.; Benson, M. C.; Bishop, L. M.; Louis, K. M.; Yeager, J. C.; Tan, Y.; Hamers, R. J. *ACS Nano* **2012**, *6*, 310–318.
- (11) Firstenberg, M.; Shivananda, K. N.; Cohen, I.; Solomeshch, O.; Medvedev, V.; Tessler, N.; Eichen, Y. *Adv. Funct. Mater.* **2011**, *21*, 634–643.
- (12) Leroux, Y. R.; Fei, H.; Noel, J.-M.; Roux, C.; Hapiot, P. *J. Am. Chem. Soc.* **2010**, *132*, 14039–14041.
- (13) Ruther, R. E.; Cui, Q.; Hamers, R. J. *J. Am. Chem. Soc.* **2013**, *135*, 5751–5761.
- (14) Bergren, A. J.; Harris, K. D.; Deng, F.; McCreery, R. *J. Phys.: Condens. Matter* **2008**, *20*, 374117.
- (15) Yan, H.; Bergren, A. J.; McCreery, R. L. *J. Am. Chem. Soc.* **2011**, *133*, 19168–19177.
- (16) Luo, L.; Choi, S. H.; Frisbie, C. D. *Chem. Mater.* **2011**, *23*, 631–645.
- (17) Poot, M.; Osorio, E.; O'Neill, K.; Thijssen, J. M.; Vanmaekelbergh, D.; Van Walree, C. A.; Jenneskens, L. W.; Van Der Zant, H. S. *J. Nano Lett.* **2006**, *6*, 1031–1035.
- (18) Nijhuis, C. A.; Reus, W. F.; Whitesides, G. M. *J. Am. Chem. Soc.* **2010**, *132*, 18386–18401. Nijhuis, C. A.; Reus, W. F.; Whitesides, G. M. *J. Am. Chem. Soc.* **2009**, *131*, 17814–17827.
- (19) Yoon, H. J.; Shapiro, N. D.; Park, K. M.; Thuo, M. M.; Soh, S.; Whitesides, G. M. *Angew. Chem., Int. Ed.* **2012**, *51*, 4658–4661.
- (20) Bonifas, A. P.; McCreery, R. L. *Nature Nanotechnol.* **2010**, *5*, 612–617.